Available online at www.sciencedirect.com
ScienceDirect
Journal of the European Ceramic Society 27 (2007) 2797–2802
www.elsevier.com/locate/jeurceramsoc

# Signature of lattice defects in far infrared reflectivity of $Ba(Mg_{1/3}Ta_{2/3})O_3$

T. Shimada [a,*], K. Touji [a], Hsiang-Lin Liu [b], Yuan-Tai Tzeng [b], Chih-Ta Chia [b], T. Kolodiazhnyi [c]

[a] *Magnetic Materials Research Laboratory, NEOMAX Co. Ltd., 2-15-17 Egawa, Shimamoto, Osaka 618-0013, Japan*
[b] *Department of Physics, National Taiwan Normal University, 88 Ting-Chou Road, Sec. 4, Taipei, Taiwan, ROC*
[c] *ICYS, National Institute for Material Science, 1-1 Namiki, Tsukuba, Ibaraki 305-0044, Japan*

Available online 24 January 2007

**Abstract**

Far infrared reflectivity spectra of $Ba(Mg_{1/3},Ta_{2/3})O_3$ prepared at several sintering temperatures were measured, and the eigenfrequencies and damping constants of the TO modes were determined. The reflectivity spectra were fitted with the four-parameter semi-quantum model. The variation in the $E_u(O_{II})$ at 222 $cm^{-1}$ and $A_{2u}(O_{II})$ at 238 $cm^{-1}$ modes in well ordered ceramics was attributed to the variation in the concentration of the B site defects. It was also found that the change in the oxygen partial pressure of the sintering atmosphere causes a change in the seventh (316 $cm^{-1}$) and eighth (352 $cm^{-1}$) modes. We attribute these changes to the oxygen site defect although we cannot evaluate the concentration of this defect at this moment. From the behavior of the damping constants it is suggested that the $Ba(Mg_{1/3}Ta_{2/3})O_3$ (BMT) attains equilibrium defect density at the heat treatment temperature of more than 1630 °C (120 h).


*Keyword:* Spectroscopy; Dielectric properties; Perovskites; Lattice defects

## 1. Introduction

$Ba(Mg_{1/3}Ta_{2/3})O_3$ (BMT) is a dielectric material possessing a high *Q* value which makes it suitable for applications as a dielectric resonator in a band pass filters for wireless communication. Recent studies on the BMT were focused on the origin of its extremely low dielectric loss. Kolodiazhnyi et al. have utilized a whispering gallery mode technique[1] to find that the least upper bound of the Qf value of the BMT is about 430 ± 20 THz. Substitution effects on the magnesium ion site on the dielectric losses have been the topic of our previous studies.[2–4] Chen et al. investigated the dielectric properties and their relation to the phonon spectra in the BMT–$Ba(Mg_{1/3}Nb_{2/3})O_3$ (BMN) system.[5] Analysis of the grain size and preparation conditions of the BMT on dielectric loss was carried out by Barber et al.,[6] Liang et al.,[7] and Ichinose and Shimada.[8] From these investigations the dielectric properties of the BMT as a microwave ceramics were roughly clarified. Recently Murata introduced a novel BMT ceramics for application in the visible range.[9] This ceramic is optically transparent and its refractive index is higher than that of many of the existing glasses.

Unlike lead-containing complex perovskites, the BMT orders easily to form a 1:2 hexagonal superstructure as confirmed by the X-ray diffraction (XRD) and transmission electron microscopy (TEM). It is generally believed that the highest degree of the 1:2 ordering warrants the lowest dielectric loss at the microwave (MW) frequency. However, according to the literature, the degree of the long-range 1:2 order evaluated from the XRD data does not always correlate well with the magnitude of the MW dielectric loss in the BMT. There are several reasons that can partially explain this discrepancy. Although the X-ray diffraction remains the most accurate technique for evaluation of the long-range 1:2 order in BMT, the experimental error of this method is high. For conventional laboratory X-rays, the error is about 2–3%, whereas for high flux neutrons or synchrotron X-rays, the error still remains at about 0.5% at best.[10] As for the TEM approach, despite the fact that HRTEM allows direct observation of the 1:2 ordered domains, analysis of the *degree* of the 1:2 ordering by the TEM electron diffraction gives only marginally qualitative information.[6] TEM provides a clear evidence of the extended lattice defects, such as dislocations and stacking faults within the 1:2 ordered BMT domains.[7] These low-dimensional defects are invisible for the XRD; however, the use of the TEM for statistical evaluation of the *density* of these defects is highly problematic.

Besides the grain boundaries and secondary phases, the $\tan\delta$ of the complex 1:2 perovskites is also affected by the

* Corresponding author. Tel.: +81 75 961 3151; fax: +81 75 962 9690.
*E-mail address:* SHIMADA.T@neomax.co.jp (T. Shimada).

0955-2219/$ – see front matter © 2007 Elsevier Ltd. All rights reserved.
doi:10.1016/j.jeurceramsoc.2006.11.005

scattering of phonons: (i) on the local imperfections (e.g., stacking faults, dislocations and anti-site lattice defects) within the 1:2 domains and (ii) on the 1:2 domain walls and anti-phase domain boundaries.[11] It is not a trivial task to separate these contributions and to distinguish the most important one. Unlike XRD, Raman and IR techniques are much more efficient in probing the local structure on the nanometer and sub-nanometer scale. Our previous studies indicated that the FIR spectra of the BMT and BMZT showed a remarkable difference among the samples having different dielectric loss.[2] These changes were attributed to the variation of the damping constants of the fourth and fifth modes in the 210–270 $cm^{-1}$ range. The important point is that these spectral changes are localized in a narrow frequency range, which, we believe, reflects the lattice dynamics associated with the B site environment. In addition, the most effective mode for dielectric loss may be specified by comparison of the vibration parameters with the Qf value at the MW range.

It has been well documented that the lattice defects can affect the MW dielectric properties of ceramics. In particular, the dielectric loss, of $Al_2O_3$ and $TiO_2$ in the MW range may vary by orders of magnitude depending on the concentration of intrinsic and extrinsic defects.[12,13] According to the theory of the phonon interaction with defects,[14] the presence of the lattice defect would change both the dispersion, $k(\omega)$, and the damping, $\gamma$, of the phonon in the otherwise perfect lattice. Hence, Raman and FTIR techniques could be particularly suitable to reveal the effect of the lattice defects on the parameters of the fundamental phonon modes. The present study is an attempt to distinguish the role of the lattice defects in the FIR reflectance spectra of the BMT.

## 2. Experimental procedure

Twenty-two BMT samples were prepared by a conventional mixed-oxide reaction process and sintered under several conditions in an electric furnace. To prepare the BMT ceramics for the far infrared measurement, extremely high purity reagents of magnesium and tantalum oxides and barium carbonates were used. The raw material consisting of oxides and carbonates were weighed to yield stoichiometric composition, mixed by ball mill using yttria stabilized zirconia balls in deionized water and calcined for 4 h at 1300 °C in air after drying. The calcined powder was then subjected to ball-milling again until the particle showed narrow distribution and about 1 μm in average particle size. The ground powders were granulated with PVA and pressed into pellets of 12 mm in diameter under a pressure of about 120 MPa using uniaxial pressing. The pellets were sintered at 1530, 1580, 1630 and 1680 °C for 5, 20, 60 and 120 h under $P_{O_2} = 0.8$ atm. Several pellets were sintered at 1580, 1630 and 1680 °C for 120 h at $P_{O_2} \approx 0.01$ atm in order to investigate the influence of the oxygen vacancies. The heating rate during sintering was fixed at 400 °C/h in order to obtain the thermochemically reliable samples. The sintered pellets were sliced to a height of about 5 and 10 mm and their permittivity and Qf value were measured by Hakki and Coleman's open resonator method in the microwave range using a network analyzer (HP 8720D). After the measurement of the dielectric properties, the pellets were thinned down to less than 0.1 mm to prepare the samples for the TEM observation using JEOL 3010 EX. Final thinning was done by a focused ion beam and perforation was achieved by the standard ion milling. For optical spectroscopy the surfaces of the sintered samples were wet polished using 0.5 μm diamond slurry until the surface roughness ($R_a$) was less than $6.0 \times 10^{-4}$ μm. To avoid the influence of the surface contamination on the IR measurement the samples were washed with acetone in an ultrasonic bath. Far-infrared reflection spectra were measured at room temperature with a Fourier transform infrared spectrometer (FT-IR; Bruker IFS 66V/S) having a SiC glow bar lamp and Au reflector as a reference. The incident angle of radiation was 11° and the spectra resolution was 1.0 $cm^{-1}$. The frequencies of the lattice vibration were estimated by the fitting of the data with the four-parameter semi-quantum model (FPSQ).

## 3. Results and discussion

Fig. 1a shows effect of the sintering time on the dielectric permittivity of BMT. The permittivity of the BMT obtained in this experiment is in the range of 11.3–24.8. The permittivity of the samples sintered at relatively low temperature and short

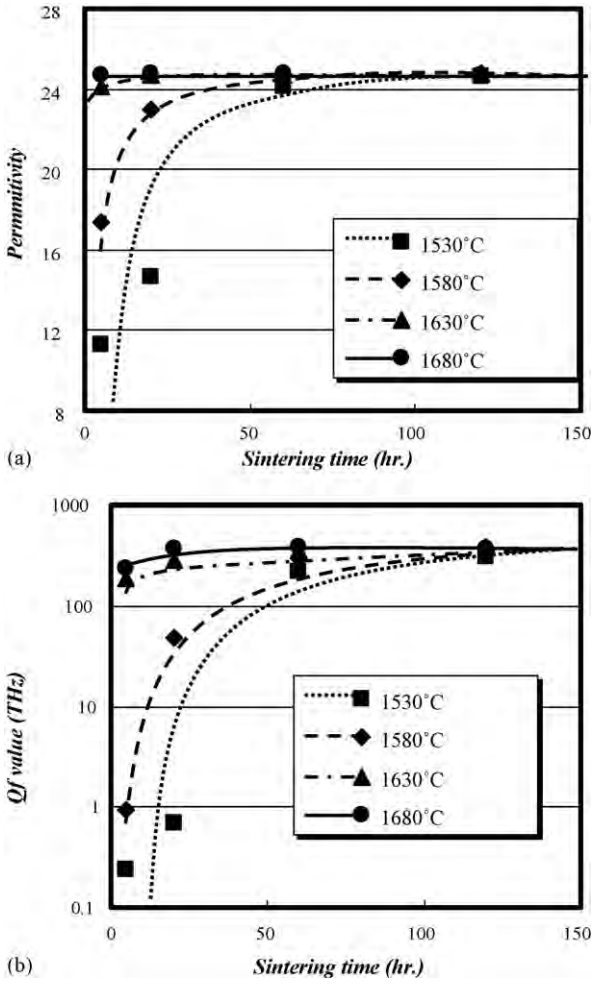


Fig. 1. (a) Permittivity change of BMT with sintering temperature and time. (b) Qf value change of BMT with sintering temperature and time.

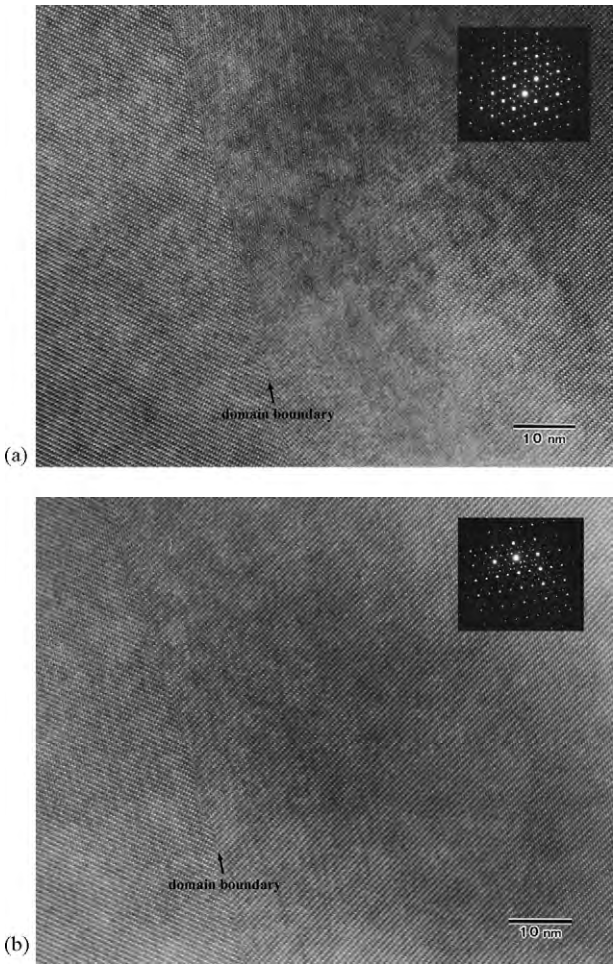


Fig. 2. HRTEM images of BMT sintered for 120 h: (a) sintering temperature, 1530 °C and (b) sintering temperature, 1680 °C.

treatment time is low due to the lower density of these samples. Fig. 1b shows improvement of the Qf value with sintering time. This dielectric loss ($1/Q$) includes the loss caused by the scattering on grain boundary, domain walls, secondary phases and the lattice defects. According to the investigation by Ichinose and Shimada,[8] the effect of the interruption of the 1:2 ordering at the grain boundary vanishes in the BMT having relatively high Qf value. It was confirmed that the $\tan\delta$ of the samples possessing high Qf value of more than 250 THz was mainly controlled by the lattice defects. HRTEM images of the samples sintered at 1530 and 1680 °C for 120 h are shown in Fig. 2a and b, respectively. We do not observe any significant difference between the microstructure and electron diffraction pattern of the BMT samples sintered at 1530–1680 °C for 120 h. Therefore, it is reasonable to assume that the dielectric loss of all samples sintered for 120 h at each temperature are caused mainly by the lattice defects.

As mentioned in introduction, the B site disorder influences the infrared reflectivity of the BMT. This disorder can be viewed as $Ta_{Mg}$ and $Mg_{Ta}$ anti-site lattice defects embedded randomly into the 1:2 ordered matrix. The influence of these defects is most pronounced in the fourth and fifth oxygen vibration modes. Fig. 3 shows a typical full range infrared spectrum of the BMT.

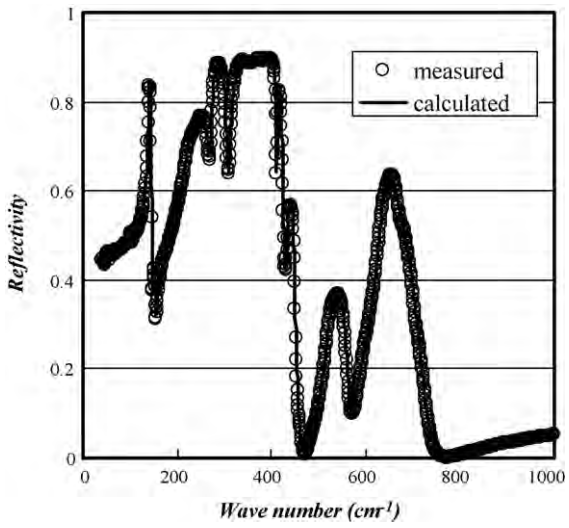


Fig. 3. Typical far infrared reflectivity of BMT, this spectrum was obtained by sintering at 1680 °C for 120 h.

The reflectivity spectra in the frequency range of 210–270 $cm^{-1}$ are compared for the BMT sintered at 1530–1680 °C for 120 h in Fig. 4. As shown in Fig. 4, the spectrum of the BMT sintered at 1530 °C is clearly divided into two peaks. In addition in order to confirm the spectrum variation until the BMT attains equilibrium, the sintering time dependence of the spectrum is also shown in Fig. 5. These modes are strongly affected by the state of the Ta site as they reflect the O–Ta–O bending.[15] The reflectivity variation in Fig. 4 indicates that the degree of the B site ordering affects the damping constants of each mode. The

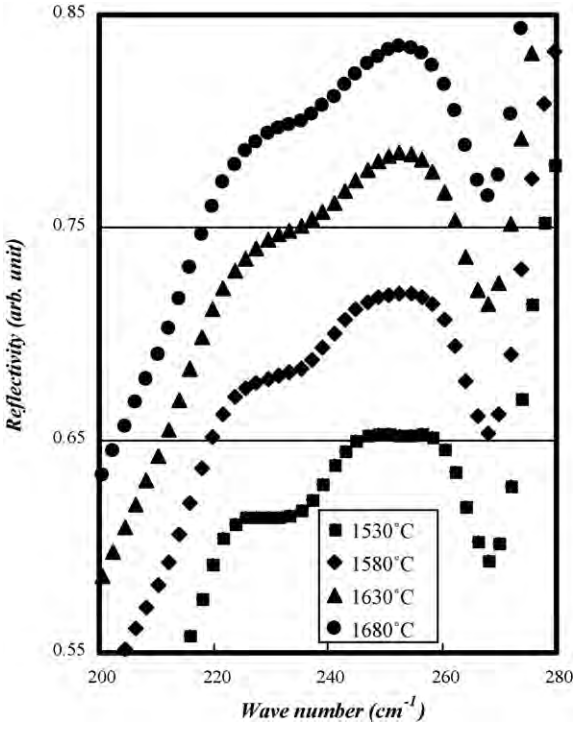


Fig. 4. Variation of far infrared reflectivity observed in fourth and fifth modes with sintering temperature, all materials were sintered for 120 h.

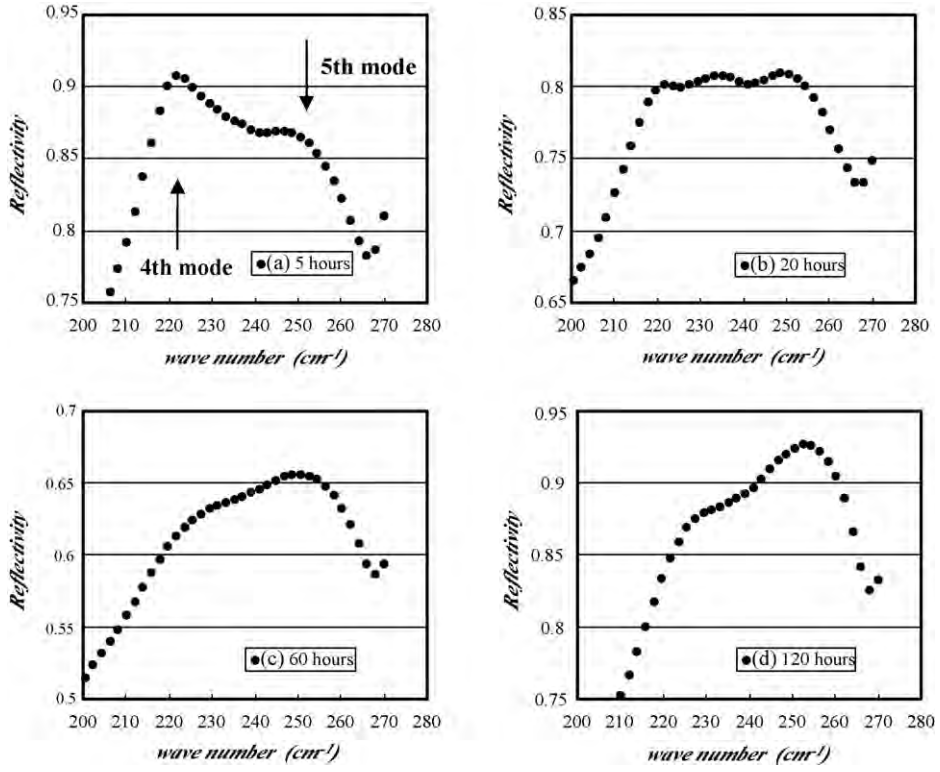


Fig. 5. Sintering time dependence of far infrared reflectivity in the range of 200–280 $cm^{-1}$, these samples were sintered at 1620 °C.

damping constant can be considered proportional to the number of the defective oscillators. The LST relation shows that the permittivity increases with the oscillator density, and in the narrow range of the permittivity, the oscillator density increases linearly. The real part of the permittivity in the IR region is given by

$$\varepsilon' = \varepsilon_\infty + \frac{(\varepsilon_0 - \varepsilon_\infty)(\omega_{TO}^2 - \omega^2)\omega_{TO}^2}{(\omega_{TO}^2 - \omega^2)^2 + \omega^2\gamma_{TO}^2}, \quad (1)$$

where $\gamma_{TO}$ is a damping constant of the TO lattice vibration. Near the resonant frequency $\omega_{TO}$ the permittivity is proportional to $1/\gamma_{TO}^2$. Therefore, the number of defects is approximately proportional to $1/\gamma_{TO}^2$. If the defect concentration on the Ta site reaches an equilibrium state during the heat treatment, the damping constants would reflect the equilibrium defect concentration. The defect concentration of the equilibrium state ($n_{eq}$) is given by

$$n_{eq} = N_i \exp\left(-\frac{\Delta g_d}{2kT}\right), \quad (2)$$

where $N_i$ is the total number of B site ions, $\Delta g_d$ the formation energy of the B site defect, $k$ is the Boltzmann constant and $T$ is the temperature. Thus, knowing the equilibrium defect concentration, the B site defect formation energy can be determined. The damping constants were determined by fitting the reflectivity with the FPSQ model using Eq. (3):

$$\varepsilon = \varepsilon\infty\prod_{j=1}^{16}\frac{\omega_{jLO}^2 - \omega^2 + i\omega\gamma_{jLO}}{\omega_{jTO}^2 - \omega^2 + i\omega\gamma_{TO}} \quad (3)$$

where $\omega_{LO}$ and $\gamma_{LO}$ are the resonant frequency and the damping constant of the LO mode. The actual permittivity can be divided into two terms: one term is coming from ordered crystal vibration and another one coming from disordered crystal vibration:

$$\varepsilon_{actual} = (N - n_d)\sum \varepsilon_{ord} + n_d \sum \varepsilon_{dis} \quad (4)$$

where $N$ is the total number of oscillators, $n_d$ the number of defective oscillators, $\varepsilon_{ord}$ the permittivity of ordered crystal and $\varepsilon_{dis}$ is the disordered one. The damping constant determines the shape of the spectrum and $n_d$ determines the relative contribution of the defective oscillators in the $\varepsilon_{actual}$. If the damping constant of the defective oscillator alters the shape of the reflectivity spectrum, the effect of the damping constant will remarkably appear in the spectrum. However, the damping constant of the defective oscillator will cause no change to the spectrum if the actual permittivity shows no difference from the perfectly ordered BMT.

The obtained spectrum is fitted using Eq. (3) and the damping constant can be calculated as if only one oscillator contributes to the reflectivity spectrum. The damping constant obtained from the reflectivity data should be called "apparent damping constant". In our previous study it was reported that the apparent damping constant of the fourth mode increased with the sintering time.[11] It was found that the intensity change in the spectrum has originated from the degree of the B site ordering. Since the apparent damping constant of the fifth mode decreased with sintering time although increasing the apparent damping constant was expected from Eq. (1), the terms from other than damping constant will be included in the spectrum. Hence, it is considered that the fifth mode is not appropriate for the defect analysis. Therefore, it is expected that the apparent damping constant of the fourth mode in equilibrium state decreases with heat treat-

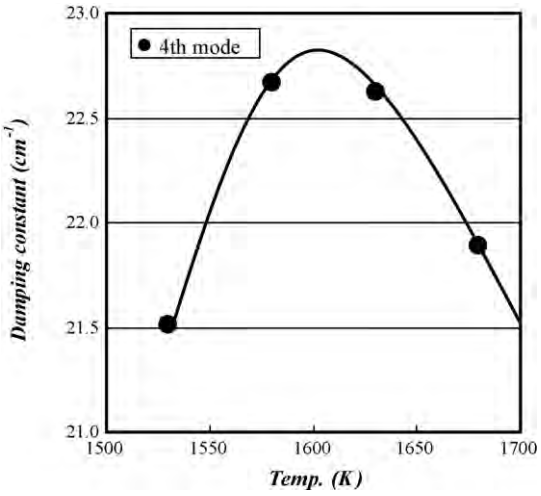


Fig. 6. Variation of apparent damping constant of fourth vibration mode for several heat treatment temperatures.

ment temperature because the defect concentration increases with heat treatment temperature. Fig. 6 shows the variation of the damping constant of the fourth mode in the BMT sintered at several temperatures for 120 h. It is obvious that the damping constant of the BMT sintered at 1530 °C does not reach an equilibrium state.

We can introduce oxygen vacancy defect in the BMT by sintering at low oxygen partial pressure. Fig. 7 shows the far infrared reflectivity of the BMT sintered at $P_{O_2} \approx 0.01$ atm at several temperatures. As shown in Fig. 7, a part of the spectrum indicated by an arrow at 335 cm$^{-1}$ protrudes with an increase in the sintering temperature. It was confirmed by the mode simulation that the reflectivity in this frequency range is caused by the

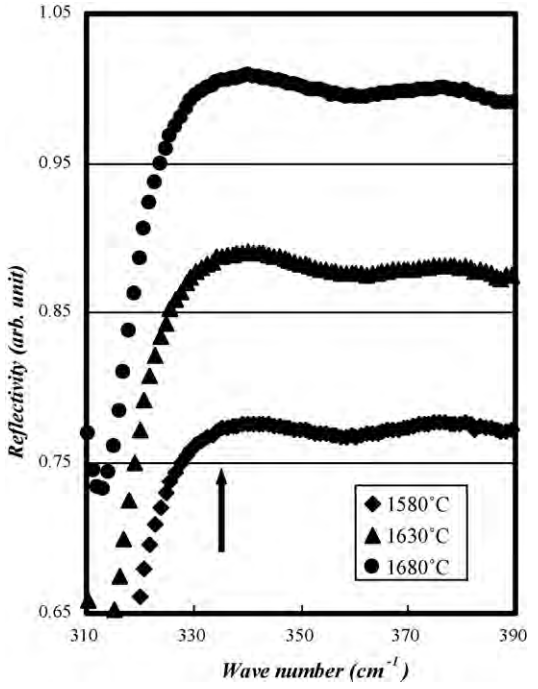


Fig. 7. Variation of far infrared reflectivity observed in vibration mode from seventh to ninth modes, all materials were sintered for 120 h.

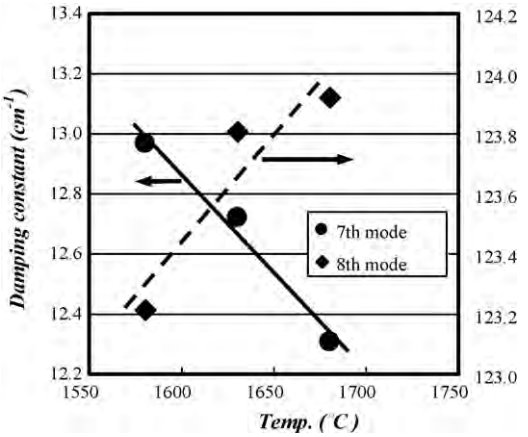


Fig. 8. Variation of apparent damping constant of seventh and eighth vibration mode in oxygen defective BMT for several heat treatment temperatures.

seventh, eighth and ninth vibration modes with $\omega_{TO} = 316$, 352 and 359 cm$^{-1}$, respectively. From our previous study,[11] these modes are hardly influenced by the B site ordering, so the apparent damping constant remains constant for samples sintered in the oxygen atmosphere. These modes are related to the Ba–O and Mg–O vibration and have small effect on the dielectric loss at microwave frequency. Since the ninth mode frequency is far from the object spectrum of the analysis, the contribution of this mode may be too small. The Mg–O stretching mode, which corresponds to the eighth mode, is the most convenient for the study of the effect of the O vacancy. Therefore, it is reasonable to use the apparent damping constants of the seventh and eighth modes to analyze the oxygen vacancy defect. Fig. 8 shows that the damping constant of the seventh mode decreased by 4.6% as the sintering temperature increased from 1580 to 1680 °C. In contrast, the damping constant of the eighth mode increased by 0.5%. At this moment we cannot propose a clear explanation of this anomalous behavior of the damping constants of the seventh and eighth modes. It is apparent however, that the concentration of the O vacancy achieved in our samples upon sintering at $P_{O_2} \approx 0.01$ atm is very small since the samples retained yellow color and no degradation of the Qf values was observed as documented in Table 1. Sintering at much lower $P_{O_2}$ may be required in order to achieve the concentration of the oxygen vacancies sufficiently high to noticeably affect the IR reflectivity.

As shown in our previous study,[10] total dielectric loss in the BMT is strongly influenced by the B site vibrations which have the resonances at 222 and 238 cm$^{-1}$ (fourth and fifth modes). It is known that the fourth and fifth modes relate to the O–Ta–O bending mode,[5] so it is expected that the dielectric loss caused by these modes may be somewhat affected by the oxygen defect. In spite of this inference, in the present experiment, the effect

Table 1
Qf value of BMT sintered for 120 h at $P_{O_2} \approx 0.01$ atm

| | Sintering temperature (°C) | | |
|---|---|---|---|
| | 1580 | 1630 | 1680 |
| Qf value (THz) | 379 | 378 | 433 |

of the oxygen defect hardly appears in the BMT sintered at $P_{O_2} \approx 0.01$ atm as if the oxygen defect does not influence the dielectric loss of the BMT at all. This controversy may result from the fact that the concentration of the oxygen vacancies obtained by sintering at $P_{O_2} \approx 0.01$ atm is too small due to the high defect formation energy. This statement, however, requires further investigations of the effect of the oxygen vacancies which are currently under way. At the present stage, it is extremely difficult to evaluate the defect formation energy because the relation between the defect concentration and the apparent damping constant is not so clear in Eq. (4). Therefore, analytical consideration of Eq. (4) is necessary to progress this study to the next step. Furthermore, in order to clarify the relation between the lattice defect and dielectric loss, we have to accumulate the data on the dielectric loss and the defect characteristics in the BMT.

## 4. Conclusion

In the present study, a qualitative analysis of the lattice defect in BMT was attempted using far infrared reflectivity spectra. It is tentatively proposed that the main contribution to the MW dielectric loss of the well processed BMT comes from the lattice point defects. The B site defect causes the change in the FIR spectrum of the fourth mode and the apparent damping constant of the sample sintered at more than 1630 °C for 120 h decreased with sintering temperature. This means that the defect concentration of the BMT has attained equilibrium at these sintering conditions. The oxygen-deficient BMT influences the FIR reflectivity of the seventh and eighth modes and the apparent damping constants of the seventh and eighth modes decrease and increase with the treatment temperature, respectively.

## References


1. Kolodiazhnyi, T., Annino, G. and Shimada, T., Intrinsic limit of dielectric loss in several $Ba(B'_{1/3}B''_{2/3})O_3$ ceramics revealed by whispering gallery mode technique. *Appl. Phys. Lett.*, 2005, **87**, 212908.
2. Shimada, T., Far-infrared reflection and microwave properties of $Ba([Mg_{1-x}Zn_x]_{1/3}Ta_{2/3})O_3$ ceramics. *J. Eur. Ceram. Soc.*, 2004, **24**, 1799–1803.
3. Shimada, T., Far-infrared studies of $Ba([Mg_{1-x}Zn_x]_{1/3}Ta_{2/3})O_3$ microwave ceramics. *J. Ceram. Soc. Jpn.*, 2004, **112**, S1571–S1578.
4. Shimada, T., Effect of Ni substitution of the dielectric properties and lattice vibration of $Ba(Mg_{1/3}Ta_{2/3})O_3$ ceramics. *J. Eur. Ceram. Soc.*, 2005, **26**, 1781–1785.
5. Chen, Y.-C., Cheng, H.-F., Lui, H.-L., Chia, C.-T. and Lin, I.-N., Correlation of microwave dielectric properties and normal vibration modes of $xBa(Mg_{1/3}Ta_{2/3})O_3$–$(1-x)Ba(Mg_{1/3}Nb_{2/3})O_3$ ceramics. *J. Appl. Phys.*, 2003, **94**, 3365–3370.
6. Barber, D. J., Moulding, K. M., Zhou, J. and Li, M., Structural order in $Ba(Zn_{1/3}Ta_{2/3})O_3$, $Ba(Zn_{1/3}Nb_{2/3})O_3$ and $Ba(Mg_{1/3}Ta_{2/3})O_3$ microwave dielectric ceramics. *J. Mater. Sci.*, 1997, **32**, 1531–1544.
7. Liang, M.-H., Hu, C.-T., Chen, H.-F., Lin, I.-N. and Steeds, J., Effect of sintering process on microstructure characteristics of $Ba(Mg_{1/3}Ta_{2/3})O_3$ ceramics and their microwave dielectric properties. *J. Eur. Ceram. Soc.*, 2001, **21**, 2759–2763.
8. Ichinose, N. and Shimada, T., Effect of grain size and secondary phase on microwave dielectric properties of $Ba(Mg_{1/3}Ta_{2/3})O_3$ and $Ba([Mg,Zn]_{1/3}Ta_{2/3})O_3$ systems. *J. Eur. Ceram. Soc.*, 2006, **26**, 1755–1759.
9. Higuchi, Y. and Tamura, H., Recent progress on the dielectric properties of dielectric resonator materials with their applications from microwave to optical frequencies. *J. Eur. Ceram. Soc.*, 2002, **23**, 2683–2688.
10. Lufaso, M., Crystal structures, modeling and dielectric property relationships of 1:2 ordered $Ba_3MM'_2O_9$ (M = Mg, Ni, Zn; M′ = Nb, Ta) perovskites. *Chem. Mater.*, 2004, **16**, 2148–2156.
11. Shimada, T., Dielectric loss and damping constants of lattice vibration in $Ba(Mg_{1/3}Ta_{2/3})O_3$ ceramics. *J. Eur. Ceram. Soc.*, 2003, **23**, 2647–2651.
12. Braginsky, V. B., Ilchenko, V. S. and Bagdassarov, K. S., Experimental observation of fundamental microwave absorption in high quality dielectric crystals. *Phys. Lett. A*, 1987, **120**, 300–305.
13. Templeton, A. *et al.*, Microwave dielectric loss of titanium oxide. *J. Am. Ceram. Soc.*, 2000, **83**, 95–100.
14. Walton, D., Phonon–defect interaction. In *Point Defects in Solids*, ed. J. H. Crawford Jr. and L. M. Slifkin. Plenum Press, 1975, p. 393.
15. Dias, A. and Moreira, L. R., Far-infrared spectroscopy in ordered and disordered $Ba(Mg_{1/3}Nb_{2/3})O_3$ microwave ceramics. *J. Appl. Phys.*, 2003, **94**, 3414–3421.